

Polarimetry of Solar System Gaseous Planets

Franco Joos, Hans Martin Schmid
(Institute of Astronomy, ETH Zurich,
Switzerland)

With the ESO 3.6-m telescope and EFOSC2 we have observed Solar System planets to investigate limb polarisation in detail. Our observations were successful and we can report the detection of limb polarisation in Uranus and Neptune. In addition spatially resolved long-slit spectropolarimetry was obtained for the first time for all the gaseous planets. The observations reveal a decrease of limb polarisation with increasing wavelength and an enhanced polarisation in the methane bands against the adjacent continuum. We describe our measurements and also discuss the diagnostic potential of such data for the investigation of the atmospheric structure of giant planets and the properties of their scattering particles.

Science motivation

Light reflected from planets is polarised. This basic property provides the opportunity to investigate planetary atmospheres by means of polarimetry. Many previous studies of Solar System planets demonstrate that polarimetry is a very powerful tool for the investigation of the atmospheric structure and the characterisation of the scattering particles. Well-known examples are the studies of the polarisation of Venus (e.g. Dollfus and Coffeen 1970), which permitted the determination of the droplet size and composition in the reflecting clouds. Other famous examples are the highly polarised poles of Jupiter which were first described by Lyot in 1929 (Lyot 1929). The polarisation at the poles is high because the radiation is reflected by Rayleigh scattering particles, while it is low at the equatorial limbs since there the light is reflected by clouds (see Figure 1). These examples illustrate well the diagnostic potential of polarimetry.

Polarimetry is also a very attractive technique for the search and investigation of extrasolar planets for three main reasons: firstly, the expected polarisation signal of the reflected light from a planet is high, on the order 5 to 50% for phase

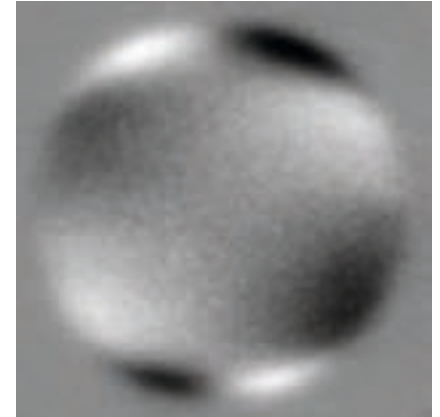
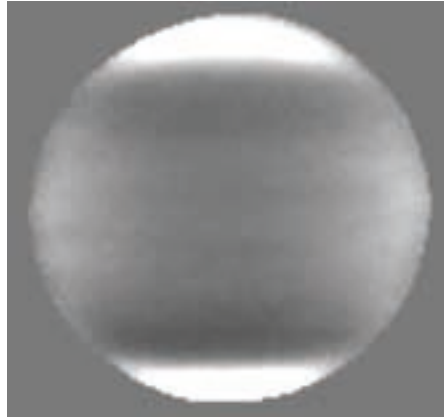


Figure 1: Imaging polarimetry of Jupiter. **Left:** the polarised Stokes Q flux, with white indicating positive (vertically) and black negative (horizontally) polarised light. **Right:** the polarised Stokes U flux (polarisation direction is rotated by 45° in a counter-clockwise direction compared with Q). Data taken with the Zurich imaging polarimeter system (ZIMPOL) at the McMath-Pierce solar telescope at Kitt Peak in a methane filter centred at 730 nm.

angles near 90° ; secondly, the reflected (= polarised) light can be distinguished from the unpolarised radiation from the central star; thirdly, the amount of polarisation provides information on the scattering particles and the atmospheric structure of the planet (see Schmid et al. 2006). Therefore, the future VLT planet finder instrument SPHERE (Spectro-Polarimetric High-contrast Exoplanet REsearch) will have a polarimetric mode in order to search for polarisation signals of extrasolar planets (Beuzit et al. 2006).

From the Earth all the giant planets are observed near zero phase angle (maximum phase angles are $\approx 11^\circ$ for Jupiter or $\approx 2^\circ$ for Neptune, for example) and essentially no polarisation is expected in integrated light. But if the planetary disc is resolved, then one can expect a limb polarisation, which arises due to a well-known second-order effect for reflecting atmospheres where Rayleigh type scattering processes are dominant (see e.g. van de Hulst 1980).

In order to understand the limb polarisation, one has to consider a back-scattering situation at the limb of a gas-rich planet, where there is locally a configuration of grazing incidence and grazing emergence for the incoming and the back-scattered photons, respectively.

Light reflected after one scattering is unpolarised, because the scattering angle is 180° . Photons undergoing two scatterings travel, after the first scattering, predominantly parallel to the surface before being reflected towards the observer by the second scattering process. The reason is that photons travelling outwards from the planet will mostly escape without a second scattering, while photons travelling inward have a low probability of being reflected towards the observer after the second scattering, but a high probability to be absorbed or to undergo multiple scatterings. Since the polarisation angle induced by a single dipole-type scattering process, like Rayleigh scattering, is perpendicular to the propagation direction of the incoming photon (which in this case is parallel to the limb), polarisation perpendicular to the limb is produced.

Limb polarisation of the giant planets has up to now hardly been investigated. Although there exist several studies based on filter polarimetry for Jupiter, and a few for Saturn, we have found no previous polarimetric observations which resolved the limb of Uranus and Neptune, nor disc-resolved spectropolarimetric measurements indicating limb polarisation. For this reason we proposed such observations with EFOSC2 at the ESO 3.6-m telescope.

Polarimetry with EFOSC2

The EFOSC2 instrument is a multi-mode Cassegrain imager and grism spectrograph which can be equipped with a Wollaston prism and a rotatable superachromatic half-wave plate for linear im-

aging polarimetry and spectropolarimetry. For linear polarimetry one measures the Stokes parameters Q and U , which are the differential intensity signals between two orthogonal linear polarisation directions according to $Q = I_0 - I_{90}$ and $U = I_{45} - I_{135}$ (where 0, 90, ... signify the polarisation direction on the sky). In EFOSC2 a Wollaston prism splits the light into the I_{\perp} and I_{\parallel} polarisation directions (relative to the orientation of the prism). The two images, called the ordinary and the extraordinary beams, are separated on the CCD by 10" or 20", respectively (see Figure 2). The two beams from the Wollaston do not overlap thanks to a special aperture mask in the focal plane with a series of open stripes (or slitlets for spectropolarimetry), whose width and separation correspond to the image separation introduced by the Wollaston beam splitter. Combining the polarimetric components with normal EFOSC2 filters or grisms then yields imaging polarimetry or spectropolarimetry, respectively (Figure 2).

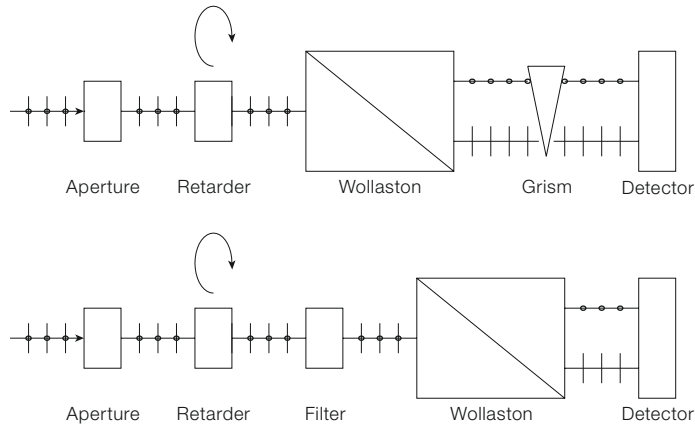


Figure 2: Schematic concept for spectropolarimetry (upper) and imaging polarimetry (lower).

Imaging polarimetry	Spectropolarimetry
Wollaston 10" stripe mask	Spectropolarimetric 20" slitlets
Half-wave plate	Half-wave plate
Broad- and narrowband filters	Wollaston prism 20"
Wollaston prism 10"	Grism ESO#5
CCD	CCD

Table 1: Set-ups for EFOSC2 imaging polarimetry and spectropolarimetry.

It is important for a high polarimetric precision that the two polarisation directions I_{\perp} and I_{\parallel} are measured simultaneously in order to avoid errors due to atmospheric seeing and transmission variations. Rotating the half-wave plate between two exposures, e.g. from 0° to 45° for Stokes Q , allows the two polarisation images to be swapped on the detector, so that differential effects in the two Wollaston beams cancel out in the polarisation signal (including the individual pixel efficiencies of the CCD). Thus, two frames taken with different retarder plate orientations yield one normalised Stokes parameter: Q/I with the half-wave plate orientations 0° and 45°; and U/I with the orientations 22.5° and 67.5° (cf. Tinbergen 1996).

The instrumental set-up for imaging polarimetry and spectropolarimetry for our planet observations is summarised in Table 1.

Figures 3 and 4 show examples of the raw frames for Uranus, taken in imaging polarimetry mode and spectropolarimetric mode, respectively. In imaging mode the ordinary and the extraordinary beams are separated by 10" in spectropolarimetric mode the separation is 20". The 20" long slit was oriented North-South over the disc of Uranus, approxi-

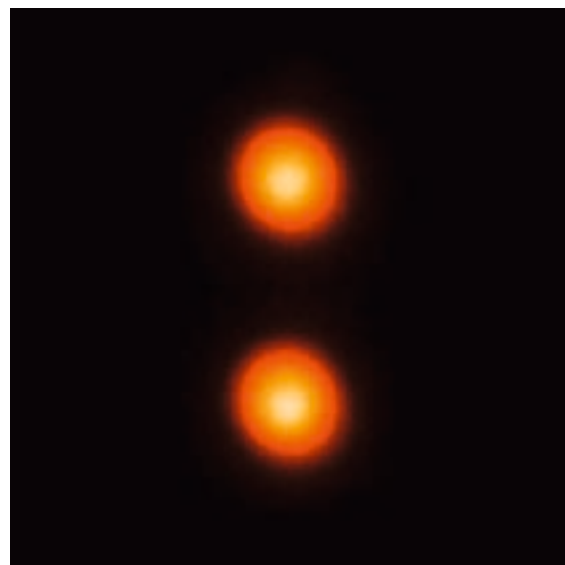


Figure 3: Raw data for an exposure of Uranus in imaging polarimetry mode. The ordinary and the extraordinary images are separated by 10". The two images are not perfectly round because Uranus showed a bright south pole and darker northern latitudes.



Figure 4: Raw data for an exposure of Uranus in spectropolarimetric mode. The deep methane absorption bands at longer wavelengths are clearly visible to the right.

mately along the planetary equator. This configuration yields long-slit spectropolarimetry, providing a centre to limb profile in intensity and polarisation for each wavelength covered by the grism.

EFOSC2 at the 3.6-m telescope is an ideal polarimetric instrument because it is attached to the Cassegrain focus and there are no strongly inclined optical components in the beam. The whole optical set-up is rotationally symmetric, so that the instrumental polarisation from the telescope and the instrument are essentially zero, at least near the optical axis. One problem of our observations was that the surface brightness of Jupiter and Saturn was too high for imaging polarimetry, even in narrowband filters. For this reason we inserted, together with some narrowband filters, an opaque mask near the pupil of EFOSC2. The mask was a self-made black plate with 28 small holes which blocked about 99% of the telescope light.

Imaging polarimetry of Uranus and Neptune

During two nights in visitor mode we were fortunate to often have subarcsec seeing conditions at the 3.6-m telescope. This allowed us to well resolve the discs of Uranus (diameter 3.5") and Neptune (2.2") and to detect the limb polarisation. The measured normalised polarisation was in the range 0.5 to 1.5% for both planets. Observations with *R* (644 nm), *i* (803 nm) and *z* (890 nm) band filters were taken for these two targets. The resulting *i*-band polarimetry is shown in Figures 5 and 6. The position of the limb, the equator and the south pole are indicated.

The Stokes *Q* and *U* images for Uranus both show a very characteristic quadrant pattern. $Q = I_0 - I_{90}$ is positive (white in the figures) or vertical at the equatorial limbs, negative (black in the figures) or horizontal at the polar limbs, and essentially zero in the centre of the planetary disc. For *U* the same pattern is apparent but rotated by 45°. Neptune shows qualitatively the same pattern. In order to obtain these *Q* and *U* maps one has to carefully align the images from the ordinary and extraordinary beam. The precision has to be better than a tenth of a

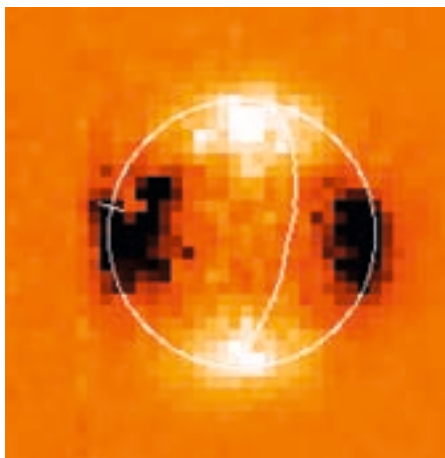


Figure 5 (above): Imaging polarimetry of Uranus in *i*-band; white corresponds to positive and black to negative polarisation. The limb is indicated by the circle, the equator by an arc and the south pole by the tick mark. **Left:** the polarised flux in the *Q*-direction with positive vertical and negative horizontal. **Right:** the polarised flux in the *U*-direction. The polarisation pattern is rotated by 45° in a counter-clockwise direction.

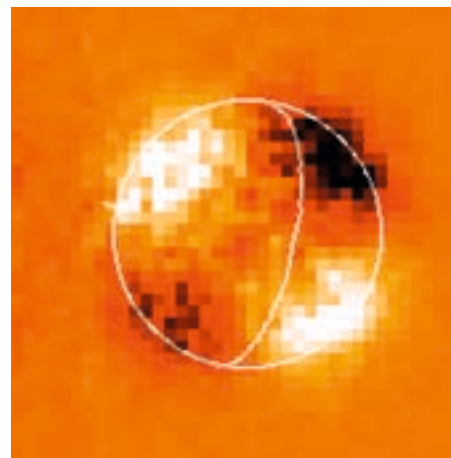
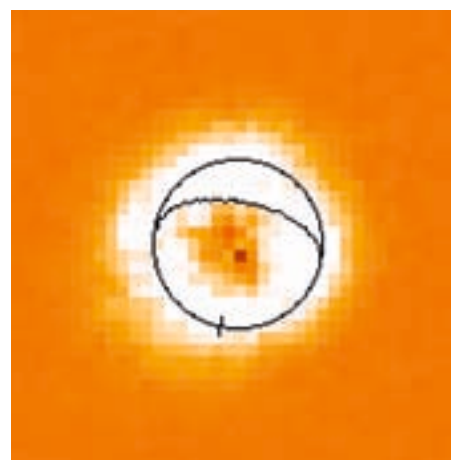
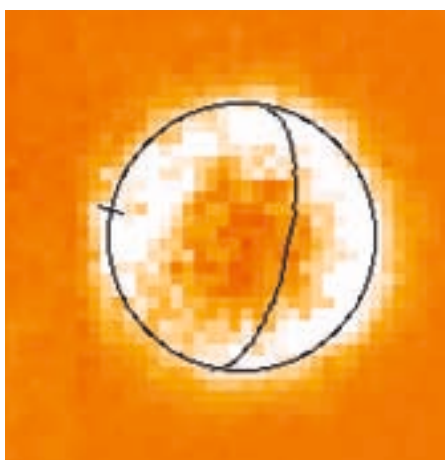


Figure 6 (below): Radial polarisation of Uranus and Neptune constructed from the *Q* and *U* images. White denotes radial polarisation and black would denote tangential polarisation, with orange as intermediate values. **Left:** Uranus in the *i*-band. **Right:** Neptune in the *R*-band.



pixel (1 pixel = 0.157"). A misalignment of one image would create a spurious positive polarisation signal at one limb and at the same time a spurious negative signal at the opposite limb.

The observed *Q* and *U* images indicate that the polarisation is high at the limb and low in the disc centre. The position angle of polarisation is perpendicular to the limb everywhere. This pattern can be better illustrated with a transformation to radial Stokes parameters Q_r and U_r , which are defined relative to the radial direction on the planetary disc. Positive Q_r indicates a radial polarisation and neg-

ative Q_r , a tangential polarisation, while $\pm U_r$ are the polarisations at $\pm 45^\circ$ orientation relative to the radial direction. The resulting Q_r images for Uranus and Neptune are shown in Figure 6. In both cases the limb polarisation is clearly visible as a bright ring with positive Q_r polarisation. The U_r images are essentially zero as there is no polarisation with a tilted orientation relative to the limb. The figures also suggest that the polarisation has a constant strength along the entire limb. This situation is unlike Jupiter (see Figure 1) or Saturn where significant limb polarisation is only observed at the poles.

For a quantitative analysis we have to take into account that the seeing-limited spatial resolution of our observations causes a degradation and cancellation in the polarisation. Our imaging polarimetry reveals that the limb polarisation decreases for both planets from the *R*- to *i*- to *z*-bands. From the Q_r maps it is also possible to derive the disc-integrated limb polarisation, which is a good parameter for comparing observations with model calculations. Unfortunately, there exists a severe lack of model calculations for limb polarisation. For this reason we compared our results with analytic calculations for Rayleigh scattering atmospheres from the 1970's and earlier, going back to the classical work of Chandrasekhar in 1950. Consulting these simple models indicates that the Rayleigh scattering layers in Uranus and Neptune have an optical depth of about $\tau = 0.2$ in the *R*-band continuum and lower for longer wavelengths. This dependence is expected as the Rayleigh scattering cross section behaves like $\sigma \propto 1/\lambda^4$. The polarisation is therefore higher for short wavelengths.

Spectropolarimetry

During the same observing run we also performed long-slit spectropolarimetry of the four giant gaseous planets. The spectropolarimetric mask consisted of a series of 20" long by 0.5" wide slitlets, aligned along a line and separated by 20" (corresponding to the beam separation of the Wollaston used for spectropolarimetry). We chose the grism ESO#5 which covers the spectral region 530 to 930 nm, providing a spectral resolution of 1.3 nm for a 1" wide slit. In this wavelength range the giant planets show a rich spectrum of weak and strong methane absorption bands. For Jupiter and Uranus we present in Figure 7 the extracted intensity (arbitrary scale) and polarisation spectrum for the limb.

For the observation of Uranus, the slit was oriented along the celestial N-S direction, covering the entire equatorial region from limb to limb. The intensity and polarisation signal were then extracted and averaged from the N and S limb regions with their high polarisation. For Jupiter the slit was aligned along the central meridian covering the northern parts

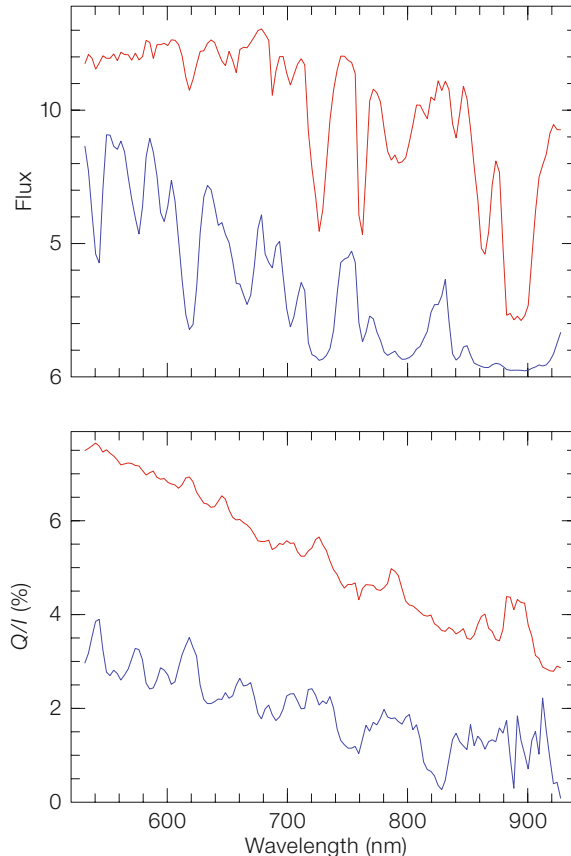


Figure 7: Spectropolarimetry for the limbs of Jupiter (red) and Uranus (blue). **Top:** flux in arbitrary units. **Bottom:** Stokes Q/I in per cent for both planets. For Uranus the polarisation signal is corrected for the degradation due to the seeing-limited resolution.

of the planet from about the centre to the limb. The diameter of Jupiter in the polar direction was 33.6". The Jupiter data in Figure 7 represent the high polarisation region at the northern limb. Further observations with different slit orientations were obtained for Jupiter and Uranus. Also Neptune and Saturn were observed in a similar way.

The data reduction turned out to be very demanding because the Wollaston introduces some dispersion perpendicular to the grism dispersion. This dispersion differs between the ordinary and extraordinary beams. Therefore, we had to align the two bent long-slit spectra to a precision of about a tenth of a pixel in the spatial direction in order to avoid spurious polarisation features due to misalignment. In the end we obtained two-dimensional long-slit spectropolarimetry providing for each wavelength disc profiles or centre-to-limb profiles for the intensity and polarisation.

First, we consider the spectropolarimetric signal of the limb. There are two general features which are present in all limb polarisation measurements of the giant planets (see Figure 7): the polarisation at the limb decreases to longer wavelengths; the polarisation is enhanced in the strong methane absorptions when compared to the adjacent higher flux regions. The overall decrease is due to the wavelength dependence of Rayleigh scattering, as already pointed out above. The enhanced polarisation in the methane bands can be explained with a two-layer model. An optically thin Rayleigh scattering layer producing the limb polarisation is located above a diffusely reflecting atmosphere or cloud layer, which reflects predominantly unpolarised light. Enhanced absorption in molecular bands efficiently reduces the unpolarised reflection of the lower layers resulting in a higher normalised polarisation for spectral regions with a low albedo.

There are significant quantitative differences in the polarisation properties of the

two planets. For example, the polarisation is very high at the poles of Jupiter, reaching values up to 9% in the V-band and the maxima in the normalised polarisation spectrum are quite narrow, due to narrow methane absorption bands. For Uranus the limb polarisation is lower, and accordingly, the polarisation maxima associated with the broad absorption bands are broader. Nevertheless, the relative polarisation enhancements in the methane bands are much more pronounced in Uranus.

Our long-slit spectropolarimetry also provides the centre-to-limb profile for the intensity and polarisation for each wavelength covered by the spectrum. For example, for Uranus we see in the strong absorption bands that the enhanced limb polarisation correlates with a limb brightening of the reflected intensity (cf. Joos and Schmid 2007). Both limb brightening and limb polarisation probe the uppermost layers of the reflecting atmospheres. Long-slit spectropolarimetry seems to be an ideal tool to investigate the structure and particle properties for these layers.

Prospects

Our polarimetric observations of the giant planets with EFOSC2 at the 3.6-m telescope demonstrate that detailed obser-

vational studies of the limb polarisation effect are possible. We have shown that a rich palette of observational parameters can be deduced from such observations and they can be used to constrain the atmospheric structure and particle properties. Additional investigations, including the still-pending analysis of our Saturn data, will further clarify the diagnostic potential of limb polarisation. Currently, an important stumbling block is the lack of detailed model calculations of the limb polarisation for realistic planetary atmospheres. Although computer codes for such model calculations exist (e.g. Braak et al. 2002), they need to be run for simulations of Earth-bound limb polarisation measurements, as presented in this article. Without such calculations we can at present only extract qualitative properties from our observations. Model calculations could significantly improve this situation.

The comparison of our data with simple (analytic) models of Rayleigh scattering atmospheres indicates that the detected limb polarisation is compatible with expectations. In general, the limb polarisation is due to Rayleigh scattering particles. They are located high in the planetary atmosphere, above layers of diffusely reflecting gas or clouds. The limb polarisation is high if the Rayleigh scattering layer is optically thick or if the penetrating

radiation is strongly absorbed in deeper layers, e.g. by methane.

For Uranus and Neptune, for which no polarimetry at large phase angles exist from space missions, we can extrapolate from the limb polarisation and estimate the expected disc integrated polarisation for phase angles near 90 degrees. We find that the polarisation must be high ($\rho > 20\%$) in the R-band. Such estimates are of interest for the interpretation of future polarimetric detections of extrasolar planets with the SPHERE VLT Planet Finder.

Acknowledgements

We are indebted to the ESO La Silla SCIOPS and the 3.6-m telescope team who were most helpful with our very special instrumental requirements. We are particularly grateful to Olivier Hainaut, Ivo Saviane and Emilio Barrios Rojas.

References

- Beuzit J. L. et al. 2006, *The Messenger* 125, 29
- Braak C. J. et al. 2002, *Icarus* 157, 401
- Dollfus A. and Coffeen D. L. 1970, *A&A* 8, 251
- Joos F. and Schmid H. M. 2007, *A&A* 463, 1201
- Lyot B. 1929, *Ann. Observ. Meudon* 8
- Schempp W. V. and Smith W. H. 1984, *Icarus* 77, 228
- Schmid H. M. et al. 2006, *IAU Coll* 200, 165
- Tinbergen J. 1996, *Astronomical polarimetry*, Cambridge University Press, 100
- van de Hulst H. C. 1980, *Multiple light scattering 2*, Academic Press



In August 2007 the Uranus ring system was almost exactly edge-on to Earth, an event which only occurs every 42 years. The two images show the Uranus system in November 2002, with the rings well displayed, and in August 2007 when the rings were edge-on and no longer visible. The image of 2002 was taken with ISAAC on the VLT while the one of 2007 was taken with NACO and made use of adaptive optics, explaining the higher resolution. The NACO image is a false colour composite based on images taken at wavelengths of 1.2 and 1.6 microns. See ESO PR 37/07 for more details.